Highly destabilized Mg-Ti-Ni-H system investigated by density functional theory and hydrogenography

C. P. Broedersz, R. Gremaud, B. Dam, and R. Griessen
Faculty of Sciences, Department of Physics and Astronomy, Condensed Matter Physics, Vrije Universiteit, De Boelelaan 1081, 1081 HV Amsterdam, The Netherlands

O. M. Løvvik
Centre for Materials Science and Nanotechnology, University of Oslo, P.O. Box 1126 Blindern, N-0318 Oslo, Norway and Institute for Energy Technology, P.O. Box 40, NO-2027 Kjeller, Norway

(Received 30 May 2007; revised manuscript received 21 October 2007; published 28 January 2008)

Using hydrogenography, we recently mapped the thermodynamic properties of a large range of compositions in the quaternary Mg-Ti-Ni-H system. The enthalpy of hydride formation of Mg-Ni alloys is significantly altered upon Ti doping. For a small range of compositions, we find a hydrogenation enthalpy $\Delta H=-40$ kJ $(\text{mol } H_2)^{-1}$, which is the desired enthalpy for hydrogen storage at moderate temperature and pressure. This enthalpy value is surprising since it is significantly less negative than the ΔH of the Mg-Ni and Mg-Ti hydrides. The nanostructure of the Mg-Ti-Ni-H films hinders a direct determination of the hydride phases involved by x-ray diffraction. Using density functional theory calculations for various hydrogenation reaction paths, we establish that the destabilization of the Mg-Ni-H system by Ti doping is due to the formation of Mg_2Ni and Ti-Ni intermetallics in the as-deposited state, which transform into a metastable Ti-doped Mg_2NiH_4 phase upon hydrogenation. The Ti-doped Mg_2NiH_4 phase can be considered as a heavily doped semiconductor.

DOI: 10.1103/PhysRevB.77.024204 PACS number(s): 61.50.Ah, 71.20.−b, 61.50.Lt, 61.66.Fn

I. INTRODUCTION

The use of hydrogen as an energy carrier in mobile application requires a suitable storage system. Solid state storage in the form of (complex) metal hydrides receives a lot of attention, since hydrogen can be stored reversibly in these materials with high volumetric and reasonable gravimetric density at a relatively low cost.[1] MgH_2, for example, has an excellent theoretical hydrogen storage capacity of 7.6 wt %. However, the enthalpy of hydrogenation is $\Delta H=-74$ kJ $(\text{mol } H_2)^{-1}$, which means that a temperature as high as 570 K is required to desorb hydrogen at atmospheric pressure. The high stability and slow absorption and desorption kinetics make this material unsuitable for application with current polymer electrolyte membrane fuel cells that operate around 350 K.

There have been many efforts to destabilize MgH_2 by alloying Mg with transition metal (TM) elements.[2–5] Very recently, metastable Mg-Ti compounds have received a lot of attention because of their good kinetics and large hydrogen storage capacity.[6,7] However, the addition of Ti does not destabilize MgH_2 significantly. The most extensively studied Mg-TM composite is the ternary hydride Mg_2NiH_4. This material has been investigated by experimentalists[3,8–11] and theorists.[12–14] Mg_2NiH_4 can theoretically store 3.6 wt % of hydrogen reversibly. The hydride formation kinetics is significantly improved compared to MgH_2, but the enthalpy of formation $\Delta H=-64$ kJ $(\text{mol } H_2)^{-1}$ of this hydride is still too negative. In order to destabilize Mg_2NiH_4, it has been alloyed with other transition metals (Ti, Cr, Mn, Fe, Co, Ni, Cu, and Zn).[15,16] Yang *et al.*[16] show in a comparative experimental study that Ti is perhaps the most promising candidate as a dopant to destabilize Mg_2NiH_4.

The remarkable properties of the Mg-Ti and the Mg-Ni systems, in addition to the work of Yang *et al.*,[16] motivated us to explore the Mg-Ti-Ni-H system using hydrogenography,[17,18] which is a new combinatorial method to study the hydrogenation properties of thin films with a compositional gradient. It exploits the large changes in optical transmission of metal alloys when they absorb hydrogen[19,20] to measure optically the equilibrium pressure of hydride formation [see Fig. 1(b)]. By doing this for several temperatures on a compositional gradient film, we can map simultaneously the enthalpy of hydride formation over thousands of alloy compositions.

Figure 1(a) shows the enthalpy of formation ΔH for the Mg-Ti-Ni-H system as measured with this technique.[17] This mapping allows us to quickly identify a range of Mg-Ti-Ni compositions with a hydride formation enthalpy of $\Delta H\approx -40$ kJ $(\text{mol } H_2)^{-1}$, commonly accepted as a desirable value for applications. The high destabilization of Mg-Ni compounds by Ti is surprising, since Ti itself forms a very stable hydride. Moreover, Ti doping of Mg_2NiH_4 reduces the hydrogen storage capacity only marginally. We determined electrochemically that 3.2 wt % (Ref. 17) of hydrogen can be stored reversibly for a compound with the composition $Mg_{0.69}Ti_{0.05}Ni_{0.26}$.

Although hydrogenography is a powerful method, it is based on thin films that are very often x-ray amorphous because of their nanoscale grains. It is, thus, difficult to determine experimentally the phases that are formed in the as-deposited and hydride states of the system. The destabilization mechanism of Ti has, therefore, been elusive.

We present in this paper a theoretical approach in which we model likely hydrogenation scenarios in the Mg-Ti-Ni-H system with density functional theory. By calculating the formation enthalpy ΔH for each case and by comparing these calculations with the experimental results, we aim to single out a scenario that is most likely responsible for the observed destabilization.

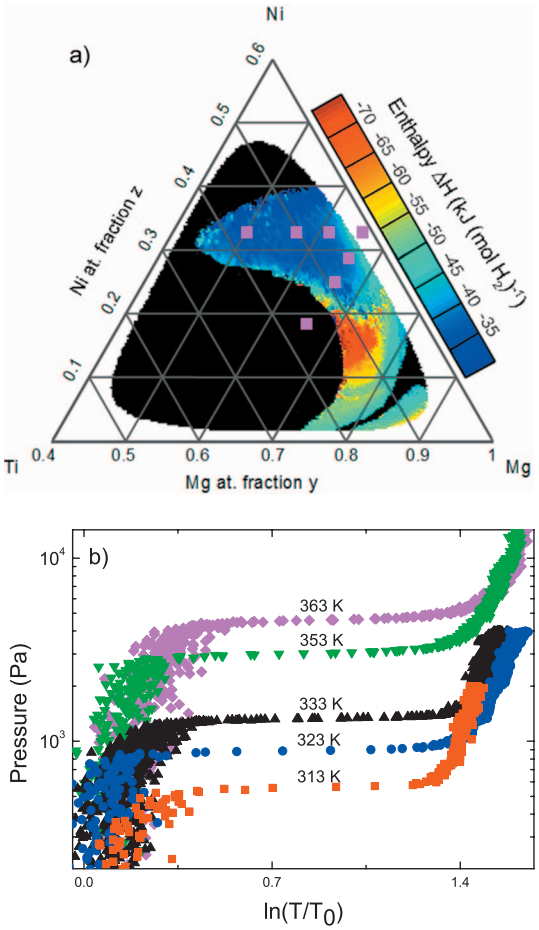

FIG. 1. (Color) (a) Hydride formation enthalpy of the Mg-Ni-Ti-H system. These results were obtained by hydrogenography (published recently by Gremaud *et al.*[17]). The dark blue region represents alloys with desirable thermodynamic properties for application as hydrogen storage materials. The pink dots indicate the compositions we describe in the present work with a DFT model. (b) The pressure-optical transmission isotherms of the composition $Mg_{0.69}Ni_{0.26}Ti_{0.05}$ for five different temperatures. The plateau is a signature of a first-order phase transition between the low-transmission metal phase and the high-transmission hydride phase and, thus, allows us to determine the equilibrium pressure of hydride formation. This particular composition is chosen because it corresponds to a destabilized hydride with an enthalpy of formation of −40 kJ $(mol\ H_2)^{-1}$ and is representative of the compositions considered in the present work.

In order to do this, we perform calculations for the compositions $Mg_2Ni_{1-y}Ti_y$ and $Mg_{2-y}NiTi_y$, with $y=0$, 1/8, 1/4, and 1/2. These are the compositions that are indicated with pink points in Fig. 1. Various scenarios are considered for the transformation from the as-deposited Mg-Ti-Ni system to Mg-Ti-Ni-H. In the as-deposited state, Ti can substitute Mg or Ni in the Mg_2Ni intermetallic, or a phase separation into Mg_2Ni and a Ti-Ni intermetallic occurs. In the hydrogenated state, mixtures of the well known phases Mg_2NiH_4, TiNiH, and TiH_2 are investigated in addition to a hypothetical mixed Mg-Ti-Ni-H phase.

Comparing calculations with the experimental results enables us to determine the phases that are likely to be formed during hydrogenation. We find that the as-deposited state is stabilized by the formation of strong Ti–Ni bonds. These bonds prevent the formation of TiH_2. In the hydride state, the Ti dopant substitutes Mg or Ni in a metastable monoclinic Mg_2NiH_4 phase without reducing the energy significantly. This scenario explains the destabilization effect of the Ti dopant. In addition to the stability calculations, we also discuss the optimized structures and the electronic structures of the Ti-doped Mg_2NiH_4 phases.

II. COMPUTATIONAL DETAILS

The calculations are done within density functional theory (DFT) at the generalized gradient approximation (GGA) level,[21] using the PBE functional.[22] We employ the projector augmented wave[23,24] formalism and a plane wave basis set with the Vienna *ab initio* simulation package (VASP).[24–26] For Mg_2NiH_4 and all Ti-doped Mg_2NiH_4 structures, we use a $2\times6\times6$ Monkhorst-Pack[27] **k**-point mesh for sampling the Brillouin zone. For Mg_2Ni and Ti-doped Mg_2Ni, we use a gamma centered $8\times8\times4$ mesh. For other structures, the spacing of the grid is at most 0.3 $Å^{-1}$. In all cases, the cutoff energy of the plane wave basis is chosen to be 700 eV. This relatively high value is used to ensure convergence within 1 meV per unit cell.

Ionic relaxations are performed by the residual minimization method with direct inversion in iterative subspace, an implementation of the quasi-Newton algorithm. Atomic positions and all cell parameters are optimized. We require the forces to be smaller than 0.05 eV/Å as a criterion for relaxation. For most of the hypothetical Ti-doped Mg_2Ni and Mg_2NiH_4, a relaxation with the conjugate-gradient algorithm was needed to achieve convergence.

It is possible that the original lattice symmetry is preserved upon Ti substitution. An appropriate DFT model would then require the use of a supercell construction to randomize the substituents and to calculate the energy while keeping the lattice symmetry fixed. However, such an approach is computationally impractical, since there are already 56 atoms in the unit cell. Our approach does not require a supercell construction and is, therefore, computationally more feasible, although it may only be an approximate description of the system. However, we do not expect this approximation to alter any of the composition dependent trends in the results.

To model the structure of the Ti-doped Mg_2Ni intermetallic, we substitute either Mg or Ni by Ti. For the single phase hydrides with compositions $Mg_{2-y}NiTi_yH_4$, we substitute the Mg atoms by Ti and, for $Mg_2Ni_{1-y}Ti_yH_4$, we substitute Ni atoms by Ti. In all cases, we have chosen to maintain the 4:3 [H]/[metal] ratio. It is conceivable that Ti substitution of Ni increases the hydrogen capacity of the material, since Ti forms a stable hydride in contrast to Ni. However, electrochemical measurements on the Mg-Ti-H system by Vermeulen *et al.*[28] demonstrate that a $Mg_{80}Ti_{20}$ compound only absorbs up to 1.6 [H]/[metal], which is significantly lower than the 2 [H]/[metal] absorbed by pure Mg. In this system, Ti apparently does not enhance the hydrogen capacity. In addition, we determined electrochemically that the Mg-Ti-Ni

TABLE I. Experimental (Ref. 33) and calculated structures of Mg_2Ni with space group $P6_222$ (180).

		a (Å)		c (Å)
Cell parameters (expt.)		5.205		13.236
Cell parameters (calc.)		5.218		13.212
Atoms		x	y	z
Mg1 (expt.)	6i	0.1620	0.324	0
Mg1 (calc.)		0.1638	0.3276	0
Mg2 (expt.)	6f	0.5	0	0.1187
Mg2 (calc.)		0.5	0	0.1168

films have a hydrogen storage capacity of 1.1 [H]/[metal],[17] which is lower than the 4/3 [H]/[metal] absorbed by pure Mg_2Ni. On the basis of the experimental results on Mg-Ti and Mg-Ti-Ni films, we decided not to increase the amount of hydrogen atoms in the unit cell.

Zero point motion (ZPM) has a significant contribution to the total energy for the hydrogen atoms. This contribution is, however, expected to be similar for Mg_2NiH_4 and the various Ti-doped Mg_2NiH_4 compounds. As we are mainly interested in energy differences, we neglect ZPM effects in the present calculations.

The enthalpy of formation ΔH is calculated by taking the difference in total electronic energy of the products and the reactants:

$$\Delta H = \sum_{products} E_p - \sum_{reactants} E_r. \quad (1)$$

In the case of the formation of Mg_2NiH_4 from Mg_2Ni and H_2, for example, ΔH is calculated per H_2 using

$$\Delta H = \frac{1}{2}E(Mg_2NiH_4) - \frac{1}{2}E(Mg_2Ni) - E(H_2). \quad (2)$$

III. CRYSTAL STRUCTURE

We use standard room temperature structures for the elemental solids.[29] The H_2 molecule is modeled using a 10 $Å^3$ cubic unit cell. To calculate the total energy of the Ti-Ni intermetallics, we relax the experimental structures of cubic Ti_2Ni [space group: $Fd\bar{3}m$ (227)],[30] martensite B19 TiNi [space group: $P2_1/m$ (11)],[31] and hexagonal $TiNi_3$ [space group: $P6_3/mmc$ (194)].[32] The optimized structures are all in close agreement with the experimental structures.

A. Ti-doped Mg_2Ni

First, we optimize the experimental structure of Mg_2Ni.[33] This hexagonal structure has space group $P6_222$ (180). Table I shows the experimental and calculated structural parameters of Mg_2Ni. The calculated parameters are in good agreement with the experiment. Using this optimized structure as a starting point, we substitute Mg or Ni by Ti, depending on the composition we wish to model. Subsequently, the doped structure is relaxed.

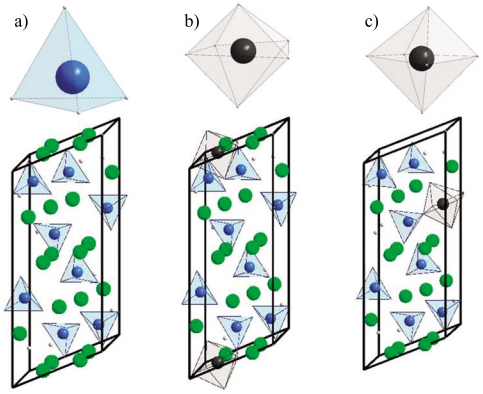

FIG. 2. (Color online) The optimized crystal structure of (a) Mg_2NiH_4, (b) $Mg_2Ni_{7/8}Ti_{1/8}H_4$, and (c) $Mg_{2-1/8}NiTi_{1/8}H_4$. We also show an enlarged picture of (a) the Ni-H and (b) and (c) the Ti-H polyhedra above the unit cell.

We model the compositions $y=0.08$, 0.17, 0.33, and 0.5 in $Mg_{2-y}NiTi_y$ and $Mg_2Ni_{1-y}Ti_y$. These compositions correspond to substituting an integer number of atoms in the 18 atom unit cell. A linear interpolation is used to obtain the total energies for $y=1/8$ and 1/4, which are needed to calculate the enthalpy of formation of the hydrides. When substituting Mg by Ti, the volume per formula unit (f.u.) decreases from 51.76 $Å^3$ ($y=0$) to 49.60 $Å^3$ ($y=1/2$), in reasonable agreement with Vegard's law. In the case of Ni substitution, we observe a volume increase to 58.74 $Å^3$ ($y=1/2$), in contradiction with Vegard's law.

B. Ti-doped Mg_2NiH_4

The low temperature phase of Mg_2NiH_4 has a monoclinic structure with space group $C2/c$ (15), which has been determined by Zolliker *et al.* on Mg_2NiD_4.[34] We take the experimental structure as a starting point and relax the structure to minimize the electronic energy. The optimized structure is shown in Fig. 2(a). We also show an enlarged image of the NiH_4 complex. This complex lies in the center of a distorted simple cubic arrangement of Mg atoms. The complexes are formed by a Ni atom surrounded by four H atoms in a nearly perfect tetrahedral arrangement. In this structure, all Ni atoms are equivalent and there are three inequivalent Mg sites. The experimental and calculated structural parameters are given in Table II. The calculated structure is in good agreement with the experimental structure and previous calculations.[13,14] Using the optimized structure of Mg_2NiH_4, we substitute either Mg or Ni by Ti and relax the resulting structure.

1. Ti substitution of Ni: $Mg_2Ni_{1-y}Ti_yH_4$

The optimized structures of $Mg_2Ni_{1-y}Ti_yH_4$ with $y=1/8$, 1/4, or 1/2 correspond to replacing one, two, or four out of the eight Ni atoms in the unit cell. For $y=1/4$, there are several ways to substitute two out of eight Ni atoms by Ti. We have chosen to investigate the two extremes; we place

TABLE II. Experimental (Ref. 34) and calculated structures of low temperature Mg_2NiH_4 with space group $C2/c$ (15).

	β (deg)	a (Å)	b (Å)	c (Å)
Cell parameters (expt.)	113.52	14.343	6.4038	6.4830
Cell parameters (calc.)	113.62	14.346	6.403	6.4849
Atoms		x	y	z
Mg1 (expt.)	8f	0.2652	0.4827	0.0754
Mg1 (calc.)		0.2632	0.4882	0.0772
Mg2 (expt.)	4e	0	0.0144	0.25
Mg2 (calc.)		0	0.0190	0.25
Mg3 (expt.)	4e	0	0.5130	0.25
Mg3 (calc.)		0	0.5208	0.25
Ni (expt.)	8f	0.1194	0.2308	0.0832
Ni (calc.)		0.1201	0.2309	0.0829
H1 (expt.)	8f	0.2113	0.2995	0.3037
H1 (calc.)		0.2112	0.3032	0.3045
H2 (expt.)	8f	0.1360	0.3163	0.8811
H2 (calc.)		0.1370	0.3185	0.8760
H3 (expt.)	8f	0.0105	0.2868	0.0537
H3 (calc.)		0.0089	0.2854	0.0513
H4 (expt.)	8f	0.1306	0.9950	0.0815
H4 (calc.)		0.1268	0.9885	0.0771

them either as closely or as distantly as possible. The choice for two neighboring Ti atoms is 27.1 kJ (mol f.u.)$^{-1}$ more stable. For $y=1/2$, there are four Ni atoms in the unit cell that are replaced by Ti. A structure with two distant pairs of neighboring Ti atoms is most stable, albeit only 5.8 kJ (mol f.u.)$^{-1}$ more stable than a structure where all Ti substitutes are adjacent.

The optimized structure of $Mg_2Ni_{7/8}Ti_{1/8}H_4$ is shown in Fig. 2(b) together with an enlarged image of the Ti-H polyhedron. For $y=1/8$ and $y=1/4$, the Ti atoms are coordinated by six hydrogen atoms in a distorted octahedron, and for $y=1/2$, the coordination increases to 7.

Table III shows several structural parameters of the relaxed structures. Substituting only one Ni atom in the unit cell by Ti ($y=1/8$) leads to a triclinic structure with space group $P1$ (1). The right angles of the monoclinic cell α and β are slightly distorted to 90.39° and 90.80°, respectively, and the volume increases by 3.5%. The angle distortions are, however, not significantly larger than the uncertainty of the method.[35] By further increasing the Ti-doping level to $y=1/4$ and $y=1/2$, we regain a monoclinic symmetry, namely, symmetry groups Pc (7) and Cc (9), respectively.

The substitution of Ni by Ti causes the unit cell volume to increase. The volume, which is slightly smaller for $y=1/4$ than for $y=1/8$, increases again significantly up to 71.44 Å^3 (f.u.)$^{-1}$ for $y=1/2$. We observe no systematic behavior in the monoclinic angle β.

TABLE III. Selected structural parameters for the optimized structure of low temperature Mg_2NiH_4, $Mg_2Ni_{1-y}Ti_yH_4$, and $Mg_{2-y}NiTi_yH_4$ for $y=1/8$, $1/4$, and $1/2$.

Compound	Space group	V/Z (Å^3)	Lattice parameters (Å)	Lattice angles
Mg_2NiH_4	$C2/2$ (27)	68.22	$a=14.3464$	
			$b=6.4026$	$\beta=113.62°$
			$c=6.4849$	
$Mg_2Ni_{1-y}Ti_yH_4$				
$y=1/8$	$P1$ (1)	70.67	$a=15.0176$	$\alpha=90.39°$
			$b=6.3291$	$\beta=112.87°$
			$c=6.4570$	$\gamma=90.80°$
$y=1/4$	Pc (7)	70.30	$a=15.1455$	
			$b=6.2318$	$\beta=112.43°$
			$c=6.4464$	
$y=1/2$	Cc (9)	71.44	$a=16.0453$	
			$b=6.0111$	$\beta=112.84°$
			$c=6.4299$	
$Mg_{2-y}NiTi_yH_4$				
$y=1/8$	$P2$ (3)	67.45	$a=14.2479$	
			$b=6.3970$	$\beta=113.11°$
			$c=6.4365$	
$y=1/4$	$P2/C$ (13)	66.70	$a=14.1561$	
			$b=6.4186$	$\beta=112.55°$
			$c=6.3460$	
$y=1/2$	$P2/c$ (13)	63.46	$a=14.3191$	
			$b=6.2507$	$\beta=115.79°$
			$c=6.2998$	

Table III reveals a remarkable feature. As the Ti-doping level increases, the unit cell swells monotonously in the direction of the a axis, while it shrinks monotonously in the b and c directions. Figure 2 helps to understand this behavior. The Ti atom strongly attracts the closest hydrogen atom of the nearby NiH_4 complexes. This causes the unit cell to contract in the bc plane. Consequently, the average H-H distance decreases from 2.6 to 2.55 Å. The Ti-H clusters are considerably larger than the Ni-H complexes, since the Ti-H distance is 20%–25% larger than the Ni-H distance. As a result, the Mg planes above and below the complex are pushed apart, leading to an increase of the lattice constant along the a axis.

2. *Ti substitution of Mg:* $Mg_{2-y}NiTi_yH_4$

There are three inequivalent Mg sites in Mg_2NiH_4. The Mg1(8f) and Mg3(4f) sites are found to be 2.9 kJ (mol f.u.)$^{-1}$ more favorable for Ti substitution than the Mg2(8f) site. There are several ways in which two or more Ti atoms can substitute the Mg1(8f) and Mg3(4f) sites in the unit cell. For $y=1/4$, the two Ti substitutes are placed closely

together since this is 8.7 kJ (mol f.u.)$^{-1}$ more stable. As in the case of Ni substitution (for $y=1/2$), placing two pairs of neighboring Ti atoms far apart is more stable than placing all Ti substitutes together. In this case, the difference in energy between the two configurations is 9.7 kJ (mol f.u.)$^{-1}$.

The optimized structure of $Mg_{2-1/8}NiTi_{1/8}H_4$ is shown in Fig. 2(c) together with an enlarged image of the Ti-H polyhedron. The coordination of H atoms around the Ti substitute increases from 6 for $y=1/8$ and $y=1/4$ to 7 for $y=1/2$.

Several structural parameters for $Mg_{2-y}NiTi_yH_4$ are shown in Table III. For all doping levels, a monoclinic unit cell is found. For $y=1/8$ in $Mg_{2-y}NiTi_yH_4$, we obtain the symmetry group $P2$ (3). Both for $y=1/4$ and $1/8$, we find the symmetry group $P2/c$ (13). No systematic behavior is observed in the monoclinic angle.

As the Ti-doping level increases, the volume per f.u. decreases monotonously from 68.22 Å^3 (f.u.)$^{-1}$ ($y=0$) to 63.46 Å^3 (f.u.)$^{-1}$ ($y=1/2$). This volume decrease is accompanied by a significant decrease in the average H-H distance from 2.61 to 2.33 Å.

IV. ELECTRONIC STRUCTURE

We calculated the total and local densities of states (DOSs) for undoped and Ti-doped low temperature Mg_2NiH_4. The structures of these compounds are discussed in Sec. III. The local DOSs of $Mg_2Ni_{1-y}Ti_yH_4$ are shown as gray filled graphs in Fig. 3 for (a) $y=1/8$ and (c) $y=1/2$, and the local DOSs of $Mg_{2-y}NiTi_yH_4$ are shown as gray filled graphs in Fig. 3 for (b) $y=1/8$ and (d) $y=1/2$. The DOS of the Ti-doped structures are plotted with respect to the Fermi level, which is displayed as a solid vertical line. To facilitate a comparison between doped and undoped Mg_2NiH_4, we show the DOS of Mg_2NiH_4 (unfilled black curve) with respect to the Fermi level of the doped compounds. The Fermi level of Mg_2NiH_4 is indicated by the dotted vertical line. The DOSs for $y=1/4$ in $Mg_2Ni_{1-y}Ti_yH_4$ and $Mg_{2-y}NiTi_yH_4$ closely resemble the DOS for $y=1/8$ and are, therefore, not shown.

The DOS of Mg_2NiH_4 is similar to previous calculations[13,14] and contains a band gap of 1.6 eV. Band structure calculations show that this gap is indirect and the optical gap is 1.7 eV, in good agreement with the experimental value.[11] This success is most probably fortuitous, since density functional theory at the GGA level is notorious for significantly underestimating band gaps.

The DOS of Mg_2NiH_4 is not effected significantly for the compounds $Mg_2Ni_{1-y}Ti_yH_4$ and $Mg_{2-y}NiTi_yH_4$ with $y \leqslant 1/4$. Therefore, we expect that the optical properties of the Ti-doped compounds are similar to the undoped compound. Ti doping is, however, expected to affect the optical properties to a certain extent, which will be discussed below separately for $Mg_2Ni_{1-y}Ti_yH_4$ and $Mg_{2-y}NiTi_yH_4$.

The Ti dopant introduces additional states in the gap between the Ni d band and the Mg s band for $Mg_2Ni_{1-y}Ti_yH_4$ [see Figs. 3(a) and 3(c)]. However, the system remains semiconducting for a doping level as high as $y=1/4$ and the gap closes for $y=1/2$. Transitions between the Ti d states and the Mg s states are expected to affect the optical properties in the near infrared.

Next we discuss the effect of Ti doping on the DOS of $Mg_{2-y}NiTi_yH_4$ [see Figs. 3(b) and 3(d)]. A fraction of the Ti d states appears as a narrow band just below the Mg s band. The Fermi level is located in the middle of the doping band, indicating metallic behavior. This seems to be in contradiction with the experiment, which has shown that thin films of these alloys become transparent upon hydrogenation. There is, however, no contradiction if the plasma frequency is sufficiently low.[36]

The plasma frequency ω_p for free electrons in a semiconducting environment can be estimated by the expression

$$\omega_p = \sqrt{\frac{ne^2}{\epsilon\epsilon_0 m^*}}, \tag{3}$$

where n is the density of charge carriers, e is the elementary charge, ϵ is the dielectric constant of the semiconductor, ϵ_0 is the permittivity of vacuum, and m^* is the effective mass of the charge carriers.

Band structure calculations (not shown) for $y=1/8$ in $Mg_{2-y}NiTi_yH_4$ along the reciprocal lattice vector corresponding to the long axis a and along the reciprocal vector along the monoclinic axis c show that the doping band appearing in the gap is composed of three overlapping Ti d bands. The first band is completely filled. The Fermi level is located in the middle of the second band, which is only half filled. Thus, there are at most three conduction electrons per unit cell, which corresponds to a charge density $n=5.5 \times 10^{27}$ m^{-3}. We estimate the effective mass by fitting the band at the Fermi level with a parabola, which gives $m^*=6 \times 10^{-30}$ kg. The dielectric function of Mg_2NiH_4 has been measured by Lohstroh *et al.*[11] for energies 0.5 eV$<E<$6.5 eV. An extrapolation to zero energy leads to $\epsilon=6.7$. Inserting these values in Eq. (3) gives $\omega_p=0.4$ eV. We, therefore, conclude that the conduction electrons introduced by the Ti doping do not contribute significantly to the optical properties of the compound in the visible part of the spectrum.

V. STABILITY PROPERTIES

Table IV shows the total energy calculated for the elemental metals, the undoped intermetallics, and the undoped hydrides. We also give the DFT total electronic energy of the H_2 molecule. These values are used for the stability analysis given below and for the calculation of the formation enthalpy of Ti-doped Mg_2NiH_4.

The compound Mg_2NiH_4 is formed by the following reaction:

$$Mg_2Ni + 2H_2 \rightarrow Mg_2NiH_4. \tag{4}$$

The hydrogenography experiments on Mg-Ti-Ni (Ref. 17) have shown that Ti doping has a dramatic effect on the ΔH of hydride formation in Mg-Ni alloys. In this section, we discuss the various ways in which Ti doping can affect both the left-hand side (as-deposited state) and the right-hand side (hydride state) of Reaction (4).

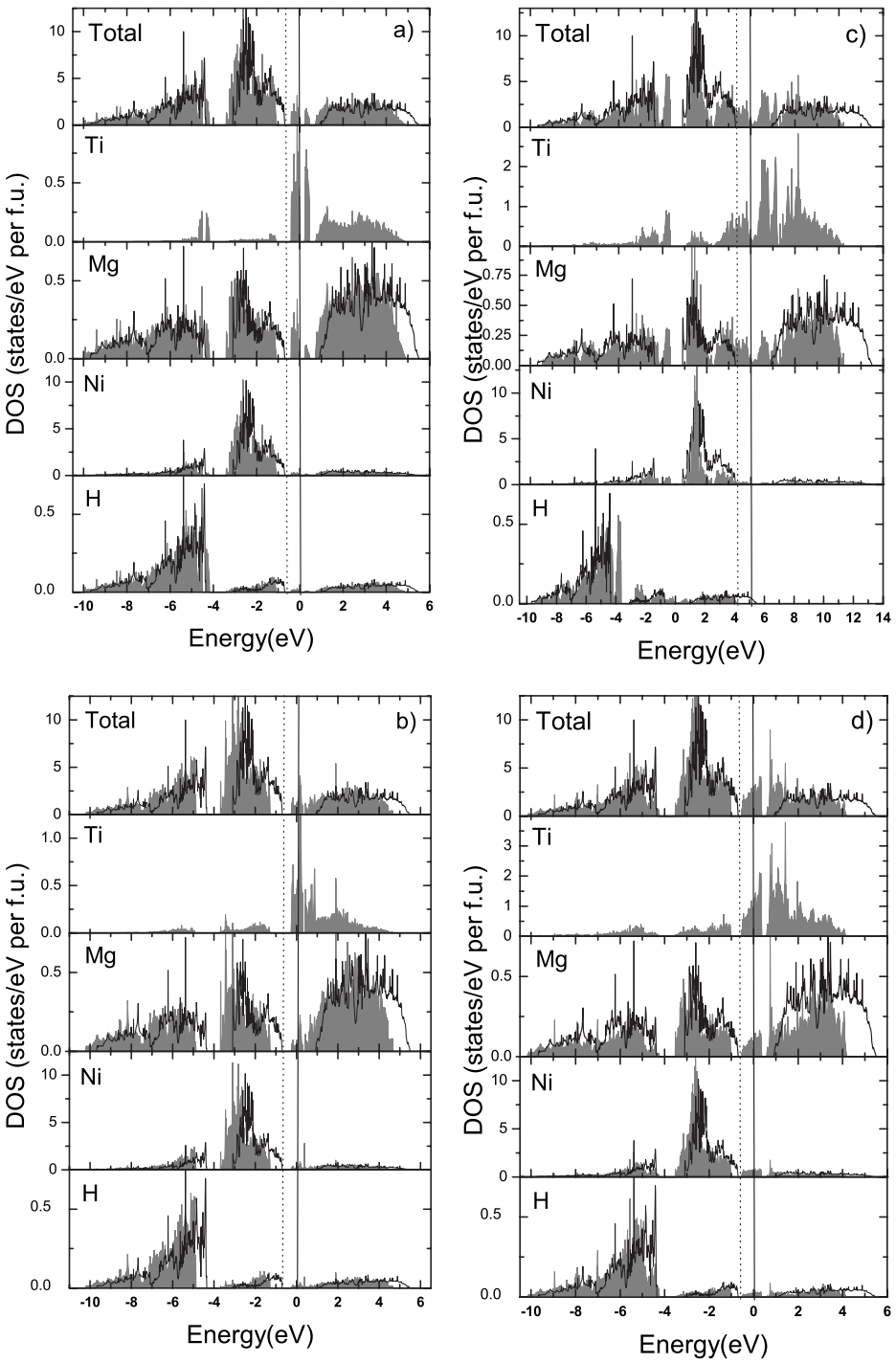

FIG. 3. Total and local densities of states with respect to the Fermi level (vertical solid line) shown as gray filled graphs of (a) $Mg_2Ni_{1-y}Ti_yH_4$ and (b) $Mg_{2-y}NiTi_yH_4$ for $y=1/8$, and of (c) $Mg_2Ni_{1-y}Ti_yH_4$ and (d) $Mg_{2-y}NiTi_yH_4$ for $y=1/2$. The total and local densities of states of Mg_2NiH_4 are also shown as an unfilled black curve with respect to the Fermi levels of the doped compounds. The Fermi level of Mg_2NiH_4 is indicated with the vertical dotted line.

A. As-deposited state

Our films are made by sputtering on a substrate at room temperature. The as-deposited state can be viewed as the solidification of hot, highly energetic atoms on a cold substrate. The two possibilities for the phases present in the as-deposited state are shown in Fig. 4. (i) The Ti dopant substitutes for Mg or Ni in the hexagonal Mg_2Ni without causing large structural changes. We refer to this case as a Ti-doped Mg_2Ni phase. (ii) The Ti atoms bind to Ni, forming a Ti-Ni intermatallic in addition to Mg_2Ni. For the latter case, we consider all three known crystalline Ti-Ni intermetallics, namely, Ti_2Ni, TiNi, and $TiNi_3$.

We calculate the total energy for the two possibilities. Figures 4(a) and 4(b) show the energy with respect to the elements for the various possible phases present in the as-deposited state for the compositions $Mg_2Ni_{1-y}Ti_y$ and $Mg_{2-y}NiTi_y$, respectively. The most striking feature of these figures is the rapid destabilization of the Ti-doped Mg_2Ni phase for increasing y in $Mg_2Ni_{1-y}Ti_y$, which is in contrast to $Mg_{2-y}NiTi_y$, where only a weak destabilization is observed.

Surprisingly, there is not a significant difference between the energies of the as-deposited state for the various Ti-Ni intermetallics. The stability of the Ti-Ni intermetallics increases with the Ni fraction. However, when a Ti-Ni inter-

TABLE IV. Calculated total energy for the pure metals, intermetallics, and hydrides. The energy is given in eV per f.u.

Compound	Energy (eV/f.u.)
Ti	−7.891
Mg	−1.554
Ni	−5.718
H_2	−6.774
Mg_2Ni	−9.503
$TiNi_3$	−27.163
TiNi	−14.464
Ti_2Ni	−22.405
Mg_2NiH_4	−24.233
MgH_2	−8.911
TiH_2	−16.127
TiNiH	−18.195

metallic is formed with a higher Ni content, less Mg_2Ni can be formed. The gain in forming the most stable intermetallic $TiNi_3$ is roughly compensated by the loss due to the decrease in Mg_2Ni amount.

Our calculations show that the formation of TiNi in addition to Mg_2Ni is energetically most favorable for all compositions. We may expect that in our sputtered films, mostly $TiNi_3$ is present for low Ti doping, and for higher Ti doping, more TiNi and Ti_2Ni are expected. Although the exact Ti-Ni intermetallic formed will depend on composition, for simplicity, we suppose TiNi for all doping levels.

A phase segregation into Mg_2Ni and the Ti-Ni intermetallics is energetically most favorable. Nevertheless, it is possible that for the compositions $Mg_{2-y}NiTi_y$ $\left(y \leqslant \frac{1}{2}\right)$ and for $Mg_2Ni_{1-y}Ti_y$ $\left(y \leqslant \frac{1}{8}\right)$, the *metastable* Ti-doped Mg_2Ni phases are formed. Therefore, we still consider this possibility for the calculation of the enthalpy of formation.

B. Hydride state

Our samples are hydrogenated by slowly increasing the hydrogen pressure to $\sim 10^5$ Pa at temperatures ranging from 313 to 363 K. The three possibilities for the phase content of the hydride state are shown in Fig. 5. (i) Mg_2NiH_4 is formed together with the interstitial hydrides TiNiH (Ref. 37) and Ti_2 NiH.[38] (ii) A Ti-doped Mg_2NiH_4 phase is formed. (iii) Mg_2NiH_4 is formed together with TiH_2.

Possibility (i) is unlikely to explain the experimental data as TiN_3, which does not form a stable hydride, is most likely to be formed in the as-deposited state for low Ti-doping levels. The other Ti-Ni intermetallics TiNi and Ti_2Ni can absorb hydrogen. However, as the Ti content increases, the ΔH of the Ti-Ni-H type hydrides becomes more negative, which cannot explain the destabilization effect of Ti found in the hydrogenography experiment.

Figure 6 shows the stability of Ti-doped Mg_2NiH_4. In this graph, the energy of Ti-doped Mg_2NiH_4 is plotted with respect to Mg_2NiH_4 and the remaining elements, and with respect to Mg_2NiH_4 and the stable hydrides including TiH_2 for the compositions $Mg_{2-y}Ni_1Ti_yH_4$ and $Mg_2Ni_{1-y}Ti_yH_4$ ($y \leqslant 1/2$). The compounds $Mg_{2-y}Ni_1Ti_yH_4$ and $Mg_2Ni_{1-y}Ti_yH_4$ are both stable with respect to Mg_2NiH_4 and the elements.

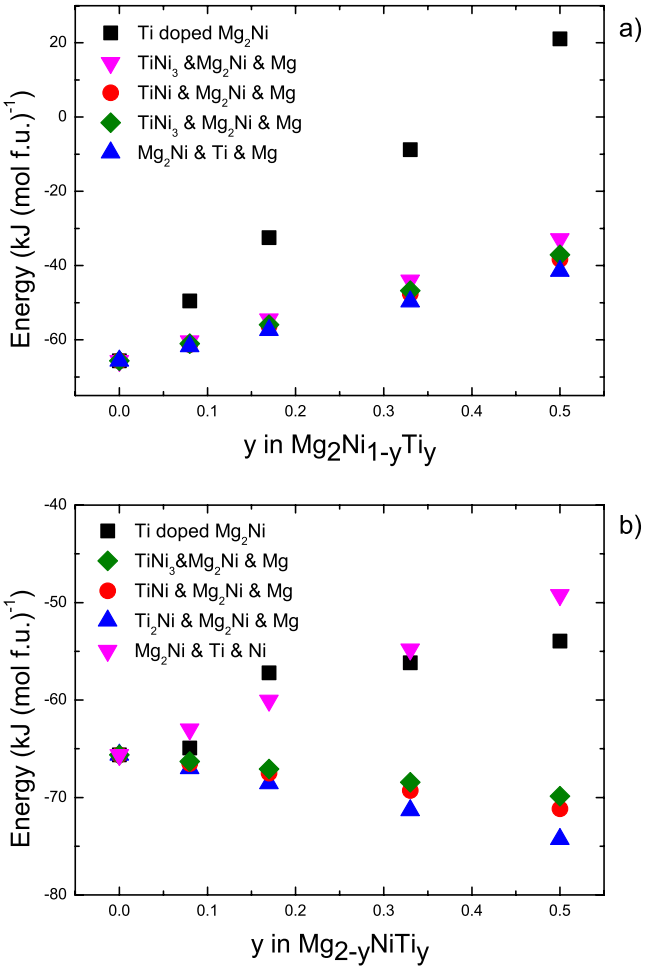

FIG. 4. (Color online) The energy with respect to the elements of the various possibilities discussed in the text for the as-deposited state for (a) $Mg_2Ni_{1-y}Ti_y$ and (b) $Mg_{2-y}NiTi_y$.

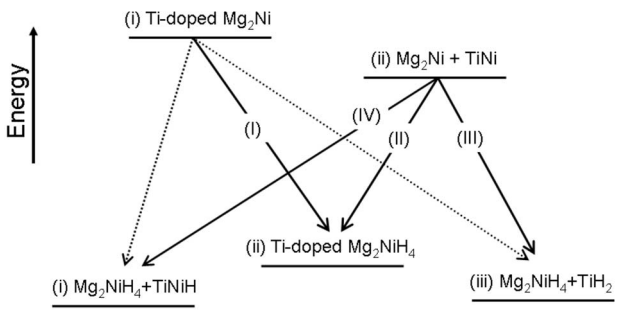

FIG. 5. Energy scheme of the various possibilities for the phase content of the as-deposited and hydride states. We also show the four considered scenarios for the reaction from the as-deposited to the hydride state with solid arrows indicated with capital roman numbers. The other reaction paths (shown with dotted arrows) cannot explain the Ti induced destabilization of Mg_2NiH_4.

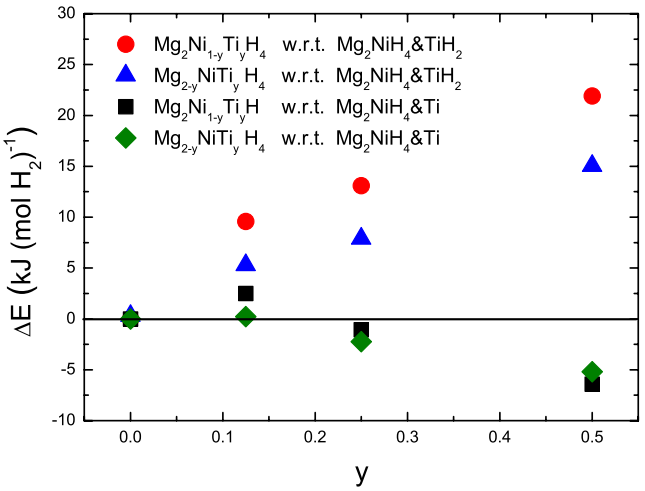

FIG. 6. (Color online) Stability of the hydride state for the compositions $Mg_{2-y}Ni_1Ti_yH_4$ and $Mg_2Ni_{1-y}Ti_yH_4$ $(0 \leqslant y \leqslant 1/2)$. The energy of the Ti-doped Mg_2NiH_4 phases is shown with respect to the energy of Mg_2NiH_4 and TiH_2 (red circles and blue triangles), and with respect to the energy of Mg_2NiH_4 and Ti (black squares and green diamonds).

DFT calculations do not incorporate temperature effects. We expect that the metastable Ti-doped Mg_2NiH_4 phases become more stable at a finite temperature due to the entropy of mixing. In addition, since the experiments are carried out around room temperature, a full segregation of the system may be kinetically hampered. We can, therefore, not rule out that the metastable Ti-doped Mg_2NiH_4 phase [possibility (iii)] forms in our hydrogenated films.

C. Calculated enthalpy of hydrogenation compared to experiment

The various possibilities for the phase content of the as-deposited and hydride states of the system give rise to different scenarios for the hydride formation (see Fig. 5). We calculate the enthalpy of formation for each likely scenario. These calculations are compared with the experimental results to see which scenario fits best. As an example, we show how we compute the enthalpy of hydride formation for the case where Mg_2Ni and Ti_2Ni react with H_2 to form the Ti-doped Mg_2NiH_4 phase:

$$\Delta H = \frac{1}{2}E(\mathrm{Mg_{2-y}NiTi_yH_4}) - \frac{1}{2}\left(1 - \frac{y}{2}\right)E(\mathrm{Mg_2Ni}) - \frac{y}{4}E(\mathrm{Ti_2Ni}) - E(\mathrm{H_2}). \quad (5)$$

We consider four different scenarios: (I) Metastable Ti-doped Mg_2Ni reacts to form metastable Ti-doped Mg_2NiH_4. Alternatively, the as-deposited state containing a mixture of Mg_2Ni and Ti-Ni intermetallics reacts to form (II) metastable Ti-doped Mg_2NiH_4 or (III) Mg_2NiH_4 and TiH_2. It is questionable whether the reaction for scenario (III) occurs in a single step or in two steps, forming first the more stable hydride TiH_2 and then Mg_2NiH_4. In the case of a multiple step reaction, we expect the presence of several plateaus in the pressure-composition isotherms. The measurements [see Fig. 1(b)], however, only exhibit a single plateau pointing in the direction of a single step reaction. This may be attributed to the large destabilization of TiH_2 due to the formation of strong Ti-Ni bonds in the as-deposited state. We, therefore, assume that the hydride formation reaction for scenario (III) occurs in a single step. We also consider a scenario (IV), where Mg_2Ni and a Ti-Ni intermetallic form a Ti-Ni hydride and Mg_2NiH_4. Such a calculation is, however, not straightforward since the type of Ti-Ni intermetallic and hydride formed depends on y. We assume, for simplicity, that for all compositions, the intermetallic TiNi and the hydride TiNiH are formed. This calculation results in a ΔH, which forms an upper bound because Ti_2Ni forms a more stable hydride.

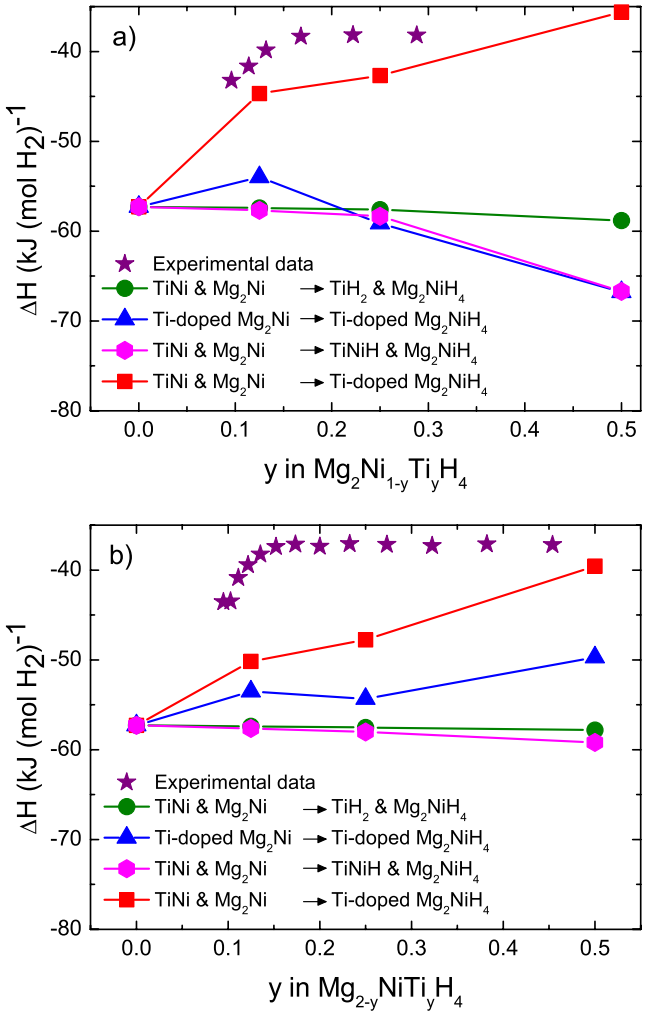

FIG. 7. (Color online) Enthalpy of formation measured by "hydrogenography" (purple stars) and calculated with density functional theory for the various scenarios discussed in the text for the compositions (a) $Mg_2Ni_{1-y}Ti_y$ and (b) $Mg_{2-y}NiTi_y$. The calculated points are connected as a guide for the eye.

Figure 7 shows the enthalpy of formation of (a) $Mg_2Ni_{1-y}Ti_yH_4$ and (b) $Mg_{2-y}Ni_1Ti_yH_4$ measured with hydrogenography (stars), and for the four scenarios calculated with density functional theory. The enthalpy of formation of undoped Mg_2NiH_4 we calculated, $\Delta H = -57.3$ kJ $(\mathrm{mol\ H_2})^{-1}$,

agrees reasonably with the measured bulk value −64.3 kJ $(\text{mol } H_2)^{-1}$.[3] Figure 7(a) shows that for compositions $Mg_2Ni_{1-y}Ti_yH_4$, only scenario (II) (TiNi and $Mg_2Ni \rightarrow$ Ti-doped Mg_2NiH_4) exhibits an increasing trend in ΔH, in quantitative agreement with the experimental data. For the compositions $Mg_{2-y}Ni_1Ti_yH_4$, we also find that scenario (II) (TiNi and $Mg_2Ni \rightarrow$ Ti-doped Mg_2NiH_4) agrees best. In this case, scenario (III) (Ti-doped $Mg_2Ni \rightarrow$ Ti-doped Mg_2NiH_4) also shows a small increasing trend, but the quantitative agreement with experiment is poor in comparison to scenario (II).

In summary, our calculations show that a reasonable agreement with experiment is found for a scenario containing Mg_2Ni and TiNi in the as-deposited state and a Ti-doped Mg_2NiH_4 phase in the hydride phase. The quantitative agreement between theory and experiment is considerably better for $Mg_2Ni_{1-y}Ti_yH_4$ than for $Mg_{2-y}Ni_1Ti_yH_4$. If the ZPM of the hydrogen atoms is taken into account, this generally leads to a more positive ΔH,[39] since the hydrogen is more confined in the solid than in the gas. The volume increase due to hydrogen absorption is significantly smaller for $Mg_{2-y}Ni_1Ti_yH_4$ than for $Mg_2Ni_{1-y}Ti_yH_4$. We expect a greater ZPM correction for $Mg_{2-y}Ni_1Ti_yH_4$ since the hydrogen is more confined in this case. Thus, including ZPM may improve the overall quantitative agreement considerably. However, the temperature dependent energies of the hydrogen molecule and of the phonons of hydrogen in the metal may well offset the ZPM contribution. This is, however, beyond the scope of this work.

The calculations suggest that the large destabilization in Ti-doped Mg_2NiH_4 is mainly due to the formation of a Ti-Ni intermetallic in the as-deposited state and a metastable Ti-doped Mg_2NiH_4 phase in the hydride state. The reversible and fast transformation from two phases to one phase upon hydrogenation at the moderate temperatures used in the hydrogenography experiments ($313\ \text{K} < T < 363\ \text{K}$) may be enabled by the small nanometer-sized grain microstructure of the system. This beneficial microstructure prohibits us, however, from measuring the phases using x-ray diffraction techniques.

Size effects may also lead to a destabilization of the hydride. However, previous calculations on the hydrogenation enthalpy of magnesium hydride clusters showed that there is no size effect until the size approached ≈1 nm.[40] This is 2 orders of magnitude smaller than the thickness of our films, and 1 order of magnitude smaller than their typical grain size. Substrate clamping in a thin film can also destabilize the hydride with respect to its bulk value since it cannot fully expand toward its equilibrium volume. The amount of destabilization depends on the elastic properties of the system, which depend only weakly on the Ti-doping level. It is, thus, still valid to compare the experimentally observed trends with the DFT results and to draw conclusions about the most likely reaction path.

The destabilization mechanism of the Ti dopant occurs probably as follows. Ti stabilizes the as-deposited state significantly by binding strongly to Ni atoms in a TiNi-like way. When the sample is hydrogenated, the strongly bound Ti does not separate to form TiH_2. The Ti dopant is, therefore, embedded in the Mg_2NiH_4 structure and substitutes either Mg or Ni without lowering the energy of the hydride significantly. This leads to the more positive enthalpy of formation of Ti-doped Mg_2NiH_4 than of the undoped compound.

VI. CONCLUSIONS

Ab initio calculations using density functional theory at the generalized gradient level are used to compute the hydride formation enthalpy of the Ti-doped Mg_2NiH_4 system. By comparing the calculations with experimental hydrogenographic results for all likely reaction scenarios, we are able to single out one scenario.

We considered various scenarios for the transformation from the as-deposited Mg-Ti-Ni system to Mg-Ti-Ni-H. In the as-deposited state, Ti can substitute Mg or Ni in the Mg_2Ni intermetallic, or a phase separation into Mg_2Ni and a Ti-Ni intermetallic occurs. In the hydrogenated state, either a mixture of Mg_2NiH_4, TiNiH, and TiH_2, or a hypothetical mixed Mg-Ti-Ni-H phase can form. Comparison between experimental and theoretical results shows that the destabilization of Ti-doped Mg_2NiH_4 is due to the formation of a Mg_2Ni and a Ti-Ni intermetallic in the as-deposited state and a metastable Ti-doped Mg_2NiH_4 phase in the hydride state.

As Mg-Ti-Ni-H compounds have remarkable optical properties, we also considered the electronic structure of Ti-doped Mg_2NiH_4 and its implications for the optical properties. The compositions $Mg_2Ni_{1-y}Ti_yH_4$ $(y \leqslant 1/2)$ exhibit semiconducting behavior in contrast to the compositions $Mg_{2-y}NiTi_yH_4$ $(y \leqslant 1/2)$, which are metallic, albeit with a low plasma frequency. This explains why these metal hydrides are transparent in the visible part of the spectrum.

The general conclusion of the present work is that a combination of the high-throughput experimental method hydrogenography and *ab initio* methods can provide additional and important insights in complex materials such as the Mg-Ti-Ni hydrides. This type of combined efforts may be crucial for a successful and efficient search for new light-weight hydrogen storage materials.

ACKNOWLEDGMENTS

We thank D. Borsa, M. J. van Setten, and S. de Man for useful discussions. C.P.B. also gratefully acknowledges the hospitality of the University of Oslo. This work is financially supported by the Stichting voor Fundamenteel Onderzoek der Materie (FOM) and the Nederlandse Organisatie voor Wetenschappelijk Onderzoek (NWO) through the Sustainable Hydrogen Programme of Advanced Chemical Technologies for Sustainability (ACTS). Computational resources were provided by the NOTUR project.

[1] A. Züttel, Mater. Today **6**, 24 (2003).
[2] J. Didisheim, P. Zolliker, K. Yvon, P. Fischer, J. Schefer, M. Gubelmann, and A. F. Williams, Inorg. Chem. **23**, 1953 (1984).
[3] J. J. Reilly and R. H. Wiswall, Inorg. Chem. **7**, 2254 (1968).
[4] J. J. Reilly and R. H. Wiswall, Inorg. Chem. **6**, 2220 (1967).
[5] P. Zolliker, K. Yvon, P. Fischer, and J. Schefer, Inorg. Chem. **24**, 4177 (1985).
[6] D. M. Borsa, A. Baldi, M. Pasturel, H. Schreuders, B. Dam, R. Griessen, P. Vermeulen, and P. H. L. Notten, Appl. Phys. Lett. **88**, 241910 (2006).
[7] D. M. Borsa, R. Gremaud, A. Baldi, H. Schreuders, J. H. Rector, B. Kooi, P. Vermeulen, P. H. L. Notten, B. Dam, and R. Griessen, Phys. Rev. B **75**, 205408 (2007).
[8] T. J. Richardson, J. L. Slack, B. Farangis, and M. D. Rubin, Appl. Phys. Lett. **80**, 1349 (2002).
[9] S. Orimo and H. Fujii, Appl. Phys. A: Mater. Sci. Process. **78**, 1235 (2001).
[10] W. Lohstroh, R. J. Westerwaal, J. L. M. van Mechelen, C. Chacon, E. Johansson, B. Dam, and R. Griessen, Phys. Rev. B **70**, 165411 (2004).
[11] W. Lohstroh, R. J. Westerwaal, J. L. M. van Mechelen, H. Schreuders, B. Dam, and R. Griessen, J. Alloys Compd. **430**, 13 (2006).
[12] G. N. Garcia, J. P. Abriata, and J. O. Sofo, Phys. Rev. B **59**, 11746 (1999).
[13] W. R. Myers, L.-W. Wang, T. J. Richardson, and M. D. Rubin, J. Appl. Phys. **91**, 4879 (2002).
[14] U. Häussermann, H. Blomqvist, and D. Noréus, Inorg. Chem. **41**, 3684 (2002).
[15] J. Huot, S. Boily, V. Guther, and R. Schulz, J. Alloys Compd. **283**, 304 (1999).
[16] H. Yang, H. Yuan, J. Ji, H. Sun, Z. Zhou, and Y. Zhang, J. Alloys Compd. **330-332**, 640644 (2002).
[17] R. Gremaud, C. Broedersz, D. M. Borsa, A. Borgschulte, P. Mauron, H. Schreuders, J. H. Rector, B. Dam, and R. Griessen, Adv. Mater. (Weinheim, Ger.) **19**, 2813 (2007).
[18] B. Dam, R. Gremaud, C. Broedersz, and R. Griessen, Scr. Mater. **56**, 853 (2007).
[19] J. N. Huiberts, R. Griessen, J. H. Rector, R. J. Wijngaarden, J. P. Dekker, D. G. de Groot, and N. J. Koeman, Nature (London) **380**, 231 (1996).
[20] T. F. Rosenbaum and A. F. T. Hoekstra, Adv. Mater. (Weinheim, Ger.) **14**, 247 (2002).
[21] J. P. Perdew, J. A. Chevary, S. H. Vosko, K. A. Jackson, M. R. Pederson, D. J. Singh, and C. Fiolhais, Phys. Rev. B **46**, 6671 (1992).
[22] J. P. Perdew, M. Ernzerhof, and K. Burke, J. Chem. Phys. **105**, 9982 (1996).
[23] P. E. Blöchl, Phys. Rev. B **50**, 17953 (1994).
[24] G. Kresse and D. Joubert, Phys. Rev. B **59**, 1758 (1999).
[25] G. Kresse and J. Furthmüller, Phys. Rev. B **54**, 11169 (1996).
[26] G. Kresse and J. Hafner, Phys. Rev. B **47**, R558 (1993).
[27] H. J. Monkhorst and J. Pack, Phys. Rev. B **13**, 5188 (1976).
[28] P. Vermeulen, R. Niessen, and P. Notten, Electrochem. Commun. **8**, 27 (2006).
[29] C. Kittel, *Introduction to Solid State Physics* (Wiley, New York, 1996).
[30] M. H. Mueller and H. W. Knott, Trans. Metall. Soc. AIME **227**, 674 (1963).
[31] H. Morawiec, D. Stroz, T. Goryczka, and D. Chrobak, Scr. Mater. **35**, 485 (1996).
[32] F. Laves and H. um Wallba, Z. Kristallogr. **101**, 78 (1939).
[33] J. Soubeyroux, D. Fruchart, A. Mikou, M. Pezat, and B. Darriet, Mater. Res. Bull. **19**, 895 (1984).
[34] P. Zolliker, K. Yvon, J. D. Jørgensen, and F. J. Rotella, Inorg. Chem. **25**, 3590 (1986).
[35] O. M. Løvvik, S. M. Opalka, H. W. Brinks, and B. C. Hauback, Phys. Rev. B **69**, 134117 (2004).
[36] O. N. Mryasov and A. J. Freeman, Phys. Rev. B **64**, 233111 (2001).
[37] J. L. Soubeyroux, D. Fruchart, G. Lorthioir, P. Ochin, and D. Colin, J. Alloys Compd. **196**, 127 (1993).
[38] H. Buchner, M. A. Gutjahr, K. D. Beccu, and H. Saufferer, Z. Metallkd. **63**, 497 (1972).
[39] M. J. van Setten, G. A. de Wijs, V. A. Popa, and G. Brocks, Phys. Rev. B **72**, 073107 (2005).
[40] R. Wagemans, J. van Lenthe, P. de Jongh, A. van Dillen AJ, and K. de Jong, J. Am. Chem. Soc. **127**, 16675 (2005).